Dalton Transactions

Accepted Manuscript

ROYAL SOCIETY OF CHEMISTRY

www.rsc.org/dalton

Efficient and persistent cold cathode emission from CuPc nanotubes: A joint experimental and simulation investigation

Uttam Kumar Ghorai[1], Swati Das[2], Subhajit Saha[1], Nilesh Mazumder[2], Dipayan Sen[2] and Kalyan Kumar Chattopadhyay[1,2]*

[1]School of Materials Science and Nanotechnology, Jadavpur University, Kolkata 700 032, India

[2]Thin Film & Nanoscience Laboratory, Department of Physics, Jadavpur University, Kolkata 700 032, India

Abstract: In the current report, chemically synthesized copper phthalocyanine (CuPc) nanotubes are shown to exhibit unprecedentedly well cold cathode emission characteristics with turn-on field (3.2 V/μm) and stable emission during long intervals (200 min). Simulation of electric field distribution via finite element method around an isolated nanotube emitter in a manner parallel to the experimental setup (inter-electrode distance = 180 μm) exhibits good corroboration of theoretical premises with experimental findings. Obtained results strongly indicate CuPc nanotubes to be potential candidate as cold cathode emitter for electron emission based applications such as field emission displays and vacuum nano-electronic devices.

Keywords: Phthalocyanine; Nanotubes; Cold cathode emission; Organic field emitter

*Corresponding author. Tel: 91 33 2413 8917; FAX: 91 33 2414 6007.

E-mail address: kalyan_chattopadhyay@yahoo.com (K.K. Chattopadhyay.)

1. Introduction:

Semiconducting organic materials have gathered phenomenal interest in the last decades owing to their significant contributions in application oriented fields such as light emitting diodes, photovoltaic cells, non-volatile memory devices, field effect transistors [1-4] etc. Apart from the above, these materials also possess further advantages of being light weight, mechanically flexible and are able to be processed at comparatively much lower temperatures. Also, in recent past, with the advent of nanoscience and technology, one-dimensional (1D) nanostructures like, wires, rods, belts and tubes of different organic semiconductors have found themselves at the pinnacle of researchers' interests due to their very high aspect ratio, large surface area for electron transport etc. Furthermore, self-assembled organic nanostructures like metal phthalocyanines have also shown excellent transport properties and thermal stability due to their π conjugated bonds and π-π stacking respectively [5-6].

Among the fascinating class of metal phthalocyanines [7-9], CuPc is of particular interest owing to its many potential applications such as photovoltaic cells, gas sensor, field-effect transistors, photodiodes [10-14] etc. There are considerable efforts for synthesizing one dimensional (1D) CuPc by different methods. For example, Jungyoon et al. [15] and Karan et al. [16] reported fabrication of CuPc thin films and different CuPc nanostructures by vacuum evaporation technique. It is to be noted that vacuum evaporation is an intricate and complex process that requires high temperature and usage of special kind of templates. Therefore, low temperature solution routes such as self-assembly, hydrothermal or solvothermal techniques are most likely to provide a convenient edge over the above [13, 17].

Field emission properties of organic nanomaterials are well reported in literature. Organic Charge transfer complexes such as CuTCNQ (TCNQ = Tetracyanoquinodimethane)

nanorods, Cu-TCNAQ (TCNAQ = Tetracyanoanthraquinodimethane) nanowires are reported to exhibit turn-on fields of 7.1 and 5.6 V/μm along with enhancement factors of 463 and 243 respectively [18-19]. Suen et al. [20] reported the turn-on field and enhancement factor of CuPc nanofibers to be 13.6 V/μm and 130 along with a field emission stability of 30 min. Tong et al. [21] fabricated CuPc nanowires by vapor deposition method which exhibited the turn-on field of 8.1 V/μm and enhancement factor of 1347 respectively. To the best of the authors' knowledge, even though there are some prior reports concerning field emission properties of organic nanotubes such as CuTCNQ or Aligned polyaniline (PANI) nanotubes, there are no such instances for the same on CuPc in literature [22-23].

In this work, the authors report field emission characteristics of hydrothermally synthesized CuPc nanotubes for the first time. The phase purity, composition and morphology of the as synthesized samples were characterized by X-ray diffraction, X-ray photoelectron spectroscopy, Field emission scanning electron microscopy and high resolution transmission electron microscopy. A tube formation mechanism is proposed by systematic investigation of the field emission scanning electron microscopic images of the nanostructures grown at different temperatures. The effect of inter-electrode distance on field emission properties is also studied in detail. Additionally, finite element method was deployed to probe and justify the experimental results from theoretical viewpoint.

2. Experimental characterizations:

CuPc self-assembled nanorods are initially synthesized analogous to a method reported in earlier works [24]. In a typical experiment, 0.0115 gm CuPc powders (Sigma Aldrich, β-form) were dispersed in 200 ml chloroform solution and the solution was ultrasonicated for 30 minutes. After that 4-6 ml of Trifluoroacetic acid **(**CF_3COOH) was mixed into the solution and the precursor solution was stirred for 6 hr. After that, the

precipitate was collected and dried for 10 h. For synthesizing nanotubes, the obtained powder was dispersed again in ethanol solution. Finally, the resulting solution was taken in a teflon lined stainless-steel autoclave of 15 ml capacity and kept at temperature 180^0C for 20h followed by gradual room temperature cooling. As obtained solution was filtered and the precipitate was washed with ethanol followed by 8 hr drying at 60^0C. To investigate the tube formation mechanism, same hydrothermal reactions were repeated at 160^0C, 170^0C and 180^0C for 20 h.

The as prepared samples were characterized by X-ray diffraction (Rigaku-Ultima-III),field emission scanning electron microscope (FESEM, Hitachi, S-4800), transmission electron microscope (TEM, JEOL-JEM 2100), Fourier transformed infrared (FTIR, Perkin Elmer spectrum II), X-ray photoelectron spectroscopy (XPS; SPECS, Germany). The inter-electrode distance dependent field emission studies were performed in our laboratory made high vacuum field emission set up [25].

3. Results & Discussion

The chemical structures of CuPc nanotubes are analyzed by Fourier transformed IR spectra. Figure 1a shows the IR transmission spectrum in the wave number range 800-1400 cm^{-1}. The peaks at 900, 1067, 1088 and 1121 cm^{-1} can be assigned to pyrrole in plane modes and the peak at 878 cm^{-1} corresponds to the pyrrole out-of-plane modes. The peak at 1166 cm^{-1} is observed due to the presence of Cu-N bonding and those at 1286 and 1332 cm^{-1} are related to C=N-C bridge sites[26]. The confirmation of exact valence states of the constituent elements in CuPc nanotubes is further confirmed by X-ray photoelectron spectroscopy (XPS). Figure 1b shows the XPS survey scan of CuPc nanotube, which does not contain any unidentified peaks. A high-resolution spectrum of N 1s is shown in the Figure 1d, which comprises of two peaks corresponding to two groups of nitrogen atoms in different chemical environments in

the CuPc molecule. These two groups might be consisted of four innermost nitrogen atoms, which interact with the central copper ion; and the four outer most nitrogen atoms are bonded to carbon atom [27]. In Figure 1c, the peaks located at 935.2 eV and 955.1 eV are attributed to the electronic states of Cu $2p_{3/2}$ and $2p_{1/2}$ respectively. The presence of satellite peaks at ~9 eV and greater than the original major peaks successfully exhibit the presence of Cu (II) state in CuPc molecule. The crystallinity of the as prepared samples was studied by XRD using a diffractometer with Cu K_{α} radiation (λ = 0.15406 nm) operating at 40 kV and 40 mA with a normal θ - 2θ scanning. Figure 1(supporting information) shows a typical XRD pattern of the as prepared sample. It can be seen that there are two strong peaks at 2θ = 7.08 and 9.25^0, indicating the formation of β phases of CuPc nanotubes. This is in good agreement with standard JCPDS data card (number: 39-1881). Presence of no other diffraction peaks conclusively confirms formation of pure phase CuPc crystal.

The FESEM images of the as-prepared CuPc nanotubes at different magnifications are shown in figure 2a and its inset. 1D CuPc nanotubes are found to grow uniformly throughout the region with length in the range of 20-50 μm. Cross section of all the tubes was observed to be rectangular with average breadth and width ~800 and 300 nm respectively. To confirm the hollow nature of the tubes, TEM analysis was also carried out. TEM images of a single tube with different magnifications are shown in Figure 2b, which clearly show that the wall thickness of the tubes lies within the range of ~70-130 nm.

To investigate the growth mechanism of these tubes, hydrothermal synthesis was performed at various temperatures. On the basis of FESEM studies of them, a possible growth mechanism is proposed which is schematically displayed in the Figure 3. At first, with the addition of CF_3COOH, self-assembled CuPc nanorods form at room temperature, which are shown in the Figure 4a. In chloroform solution, the CF_3COO^- ions interact with the

Cu^{2+} ions of CuPc molecules and act as bridging agents for formation of the self-assembled nanorods [24]. When hydrothermal treatment is carried out at 160^0C (HT160), the individual nanorods arrange themselves in a way to form half-tubular structure (shown in figure 4b). When temperature reaches 170^0C, these half-tubular structures sew together and form single rectangular tubes by joining their edges. Finally, at 180^0C (HT180), formation of nanotubes with smooth surfaces, open ends and rectangular cross section takes place. Detailed illustration of tube formation steps is depicted in Figure 4. Non-covalent forces like π-π interaction of the phthalocyanine molecules in the solution phase seems to be the driving force toward the half-tubular structure by self assembly of the individual nanorods. Finally half-tubular structures completely transforms into rectangular nanotubes to reduce their surface energy [28-29].

Field emission characteristics were carried out in our laboratory made high vacuum system at pressure of ~ 10^{-6} mbar. In this study, a conical shaped stainless steel tip (1.5mm tip diameter) served as anode and nanotube samples glued to a conductive carbon tape worked as cathode. The anode cathode distance was made adjustable to a few hundred micrometers by means of a micrometer screw. The sample size was ~ 10 mm × 10 mm. The field emission current voltage characteristics were further analyzed by the classical Fowler Nordheim (F-N) equation [30]:

$$J = (A\beta^2E^2/\varphi) \exp(-B\varphi^{3/2}/\beta E) \quad (1)$$

where A and B are constants with values of 1.54 X 10^{-6} AV^2eV and 6.83 X 10^{-3} $V/\mu m^{-1}$ $eV^{-3/2}$ respectively, J is the current density, E is the applied field, φ is the work function of the emitting materials (which is ~ 4.7 eV for CuPc) and β is the enhancement factor relating to the following equation:

$$\beta = -B\varphi^{3/2}/S \quad (2)$$

Where S is the slope of the F-N plot (i.e. a plot of $\ln(J/E^2)$ versus 1/E obtained from the F-N equation (1).The experimental J-E curve for our sample for three different inter-electrode distances (d) is shown in figure 5**.** Also in inset of figure 5a, J-E curves in the lower field region are also shown separately. It is to be noted that there exists no standardized definition for turn-on field (E_{To}) and different researchers have defined it in different ways [31-36]. Hence, we have defined the turn-on field as the field required to obtain current density of 1 $\mu A/cm^2$ by a significant jump in the current density (inset figure 5a). Furthermore, it can be noticed that the turn-on field significantly decreases with increasing inter-electrode distances. The registered turn-on field for 120 µm, 180 µm and 240 µm are found to be 4.9 V/µm, 3.2V/µm and 2.68 V/µm respectively. It is to be noted that the magnitudes of turn-on fields and enhancement factors for our synthesized CuPc tubes are better than previously reported field emission performances of several organic and inorganic nanotube field emitters [37-39]. The enhancement factors (β) for 120 µm, 180 µm and 240 µm inter electrode distances are found to be 1067, 1300 and 1650 respectively. It is well known that the enhancement factor (β) values depend on the nanostructure morphology, aspect ratio, work function of the emitter and more importantly on the screening factor. For a tube like emitter, β value not only depends on the morphology and aspect ratio but also on the ratio of the length to the wall thickness of the cold cathode emitter [40-42]. The variation of turn-on field and enhancement factor with inter electrode distance are shown in figure 5c. It is also seen that the enhancement factor (β) values increase with increasing the cathode-anode distances. In our experiment, a conical shaped stainless steel anode was used as anode where the field lines emerging from the tip are diverging in nature. As a result, when anode cathode distance increases, the effective emission area also increase and so, more electrons can reach the collector, which increases the current density. Similar trend was reported by other group also [31]. Another important factor that might affect field emission characteristics is the space

charge effect [43] and it is created in the system for the residual gases which desorbs from the cathode due to local heating and from the anode due to electron bombardment. The active space charge generated in the vacuum system may either increase or reduce the enhancement factor. In the low field region, the β value is only related to surface geometry. But in the high field region ionizations occur and the positive ions navigate towards the cathode, thus enhancing the local electric field as well as the effective β value. Lastly, field emission stability is the one of most important parameters for device oriented applications. Figure 5d shows the variation of emission current density of CuPc nanotubes up to 200 minutes under applied field of 8.7 V/μm. No obvious drop in emission current density was observed and the emission current fluctuation was less than 8%. This may be accounted to the thermally and chemically stable character of CuPc [44] and as well as the hollow tubular geometry of CuPc nanotubes as deployed in the current experiments which may provide further help to dissipate more heat from the system [45].

To gain deeper theoretical understanding of the field emission phenomena at the level of individual nanotubes, we computationally investigated the local electric field profile of the CuPc nanotubes by a finite displacement method as implemented in ANSYS Maxwell simulation package. Calculations of electric field distribution were carried out for a single CuPc nanotube as cathode and a stainless steel electrode as anode. Simulation parameters were chosen to reflect the actual dimensions of the experimental configuration to maintain a direct analogy with the experimental counterpart. We used the following parameters to simulate the CuPc nanotubes: Length = 25 μm, breadth = 700 nm, width = 200 nm, wall thickness = 90 nm, dielectric constant k = 4.4 and dc conductivity = $3.3X10^{-10}$ S/m. A potential of 1900 V was applied to the electrodes and anode to cathode separation was maintained at 180 μm. Figure 6(a-d) show the three dimensional perspective of the models of a single hollow CuPc nanotube at 90^0, 60^0, 30^0 and 3^0 inclinations along with computed

electric field distribution as overlay. A colored coordinate (red is maximum and blue is minimum) is used to map the magnitude of the electric field on the three dimensional (3D) structure. Simulated results indicate higher field emission performance is obtained for lower angular alignments which can be readily justified as edges of rectangular nanotubes accounts for sharper field emission characteristics in such cases [46]. Field enhancement factor for each of the above models can readily be estimated from the simulated result ($\beta = F/F_M$, where, F is the maximum value of local field and F_M is the applied macroscopic field). We obtained enhancement factors of ~1005, 1109, 1247, 1346 for configurations of 6(a)-(d) respectively; in average ~1177, which is in excellent agreement with experimentally obtained results.

4. Conclusions

We have investigated the cold cathode emission characteristics of chemically synthesized CuPc nanotubes at various inter-electrode distances. Good field emission properties along with as low as 3.2 V/μm turn-on field and stable field emission for as long as 200 minutes were obtained for these samples. The dependence of field emission characteristics on inter-electrode distance is also probed in detail. Obtained field emission curves are further analyzed by Fowler-Nordheim techniques and field emission parameters such as enhancement factor etc. are calculated. Local electric field enhancement around hollow tubular geometry was also studied theoretically using finite element method. The computed values of enhancement factors from the simulated results are found to be in well agreement with the experimental observations. Obtained turn-on fields and stable field emission properties imply high suitability of these CuPc nanotubes for applications ranging from vacuum nano electronic devices to field emission display devices.

Acknowledgement:

The authors wish to acknowledge the Council of Scientific and Industrial Research (CSIR), the Government of India, for awarding a Senior Research Fellowship during the execution of the work. We thank the University Grants Commission, the Government of India, for 'University with Potential for Excellence scheme' (UPE-II).

.

References:

[1] E. L. Williams, K. Haavisto, J. Li, and G. E. Jabbour, Adv. Mater. 2007, **19**,197

[2] M. D, Perez, C. Borek, S. R. Forrest and M. E. Thompson, J. Am. Chem. Soc, 2009, **131**, 9281

[3] P. Heremans, G. H. Gelinck, R. Muller, K. J. Baeg, D. Y. Kim, and Y. Y. Noh, Chem. Mater. 2011, **23**, 341

[4] A. L. Briseno, S. C. B. Mannsfeld, S. A. Jenekhe, Z. Bao, and Y. Xia, Mater. Today 2009,**11**, 38

[5] Q. Tang, L. Jiang, Y. Tong, H. Li, Y. Liu, Z. Wang, W. Hu, Y. Liu, and D. Zhu, Adv. Mater. 2008, **20**, 2947

[6] P. Pavaskar, S. Chodankar and A. Salker, European Journal of Chemistry 2, 2011, **3**, 416

[7] W. Y. Tong, A. B. Djurisic, M. H. Xie, A. C. M. Ng, K. Y. Cheung, W. K. Chan, Y. H. Leung, H. W. Lin and S. Gwo, J. Phys. Chem. B, 2006, **110** , 17406.

[8] M. Zhang, C. Shao, Z. Guo, Z. Zhang, J. Mu,T. Cao, and Y. Liu, ACS Appl. Mater. Interfaces, 2011, **3**, 369.

[9] Z. Guo, B. Chen, M. Zhang, J. Mu, C. Shao, Yichun Liu, J. Col. Interface Sci. 2010, **348**, 37.

[10] H. Xi, Z. Wei, Z. Duan, W. Xu, and D. Zhu, J. Phys. Chem. C , 2008, **112**, 19934.

[11] N. Padma, A. Joshi, A. Singh, S.K. Deshpande, D. K. Aswal, S. K. Gupta, J. V. Yakhmi, Sens. Actuators, B, 2009, **143**, 246.

[12] F. I. Bohrer, C. N. Colesniuc, J. Park, M. E. Ruidiaz, I. K. Schuller,A. C. Kummel and W. C. Trogler, J. Am. Chem. Soc. 2009, **131,** 478.

[13] J. S. Jung, J. W. Lee, K. Kim, M. Y. Cho, S. G. Jo, and J. Joo, Chem. Mater. 2010, **22,** 2219.

[14] S. Karan and B. Mallik, Nanotechnology, 2008, **19**, 495202.

[15] J. E, S. Kim, E Lim, K. Lee, D. Cha, B. Friedman, Appl. Surf. Sci. 2003, **205,** 274.

[16] S. Karan, B. Mallik J. Phys. Chem. C, 2007, **111**, 7352.

[17] J. Li, S. Wang, S. Li, Q. Wang, Y. Qian, X. Li, M. Liu, Y. Li and G. Yang, Inorg. Chem. 2008, **47**, 1255.

[18] H. Liu, X. Wu, L. Chi, D. Zhong, Q. Zhao, Y. Li, D. Yu, H. Fuchs, D. Zhu, J. Phys.Chem. C, 2008, **112,** 17625.

[19] S. Cui, Y. Li, Y. Guo, H. Liu, Y. Song, J. Xu, J.Lv, M. Zhu, D. Zhu, Adv. Mater.2008, **20**, 309.

[20] S. C. Suen , W. T. Whang , F. J. Hou, B. T. Dai, Org. Electron. 2006, **7**, 428.

[21]. W. Y. Tong , Z.X. Li , A. B. Djurišić , W. K. Chan , S. F. Yu, Mater. Lett. 2007, **61**, 3842.

[22] H. Liu, Z. Liu, X.Qian, Y. Guo, S. Cui, L. Sun, Y. Song, Y. Li, D. Zhu, Cryst. Growth Des. 2010, **10**, 237.

[23] S. S. Patil, S. P. Koiry, P. Veerender, D. K. Aswal, S. K. Gupta, D. S. Joag, M. A. More, RSC Adv. 2012, **2**, 5822.

[24] U. K. Ghorai, S. Saha, S. Shee and K. K. Chattopadhyay, AIP Conf. Proc. 2013, **1536**, 223.

[25] A. Jha, U. K. Ghorai, D. Banerjee, S. Mukherjee and K. K. Chattopadhyay, **RSC Adv.**, 2013,**3**, 1227.

[26] H. Kato, S. Takemura, Y. Watanabe, A. Ishii, I. Tsuchida, Y. Akai, T. Sugiyama,T. Hiramatsu, and N. Nanba, J. Vac. Sci. Technol. A, 2007, **25**, 1147.

[27] A. Chunder,T. Pal, S. I. Khondaker, L. Zhai, *J. Phys. Chem. C*, 2010, **114**, 15129.

[28] C. Zhao, Z. Wang, Y. Yang, C. Feng, W. Li, Y. Li, Y. Zhang, F. Bao, Y. Xing,X. Zhang, and X. Zhang, Cryst. Growth Des. 2012, **12**, 1227.

[29] Y. Huang, R. Yuan and S. Zhou, J. Mater. Chem., 2012, **22**, 883

[30] R. H. Fowler, L. Nordheim, Proc. R. Soc. Lond. A, 1928, **119**, 173.

[31] A. N. Banerjee and S. W. Joo, Nanotechnology, 2011, **22**, 365705.

[32] S. Neupane , M. Lastres , M. Chiarella , W. Li , Q. Su ,G. Du, Carbon, 2012, **50,** 2650.

[33] B. K. Gupta, D. Haranath, S. Chawla, H. Chander,V. N. Singh and V. Shanker, Nanotechnology, 2010, **21,** 225709.

[34] V. S. Kale, R. R. Prabhakar, S. S. Pramana, M. Rao, C. H. Sow, K. B. Jinesh and S. G. Mhaisalkar, Phys. Chem. Chem. Phys., 2012, **14**, 4614.

[35] V. S. Kale, B. R. Sathe, A. Kushwaha, M. Aslam andM. V. Shelke, Chem. Commun., 2011, **47**, 7785.

[36] S. S. Patil, P. Jha, D.K. Aswal, S.K. Gupta, J. V. Yakhmi, D. S. Joag and M. A. More, Polym. Adv. Technol. 2012, **23** 215.

[37] J. Cheng, Y. Zhang, and R. Guo, J. Appl. Phys. 2009, **105**, 034313.

[38] C. C. Wang, K. W. Wang and T. P. Perng, Appl. Phys. Lett. 2010, **96**, 143102.

[39] J. Lin, Y. Huang, C. Tang, Y. Bando, J. Zouc and D. Golberg, J. Mater. Chem., 2012, **22**, 8134.

[40] C. Ouyang, X. Qian, K. Wang and H. Liu, Dalton Trans., 2012, **41**, 14391.

[41] G. Li, Y. Li, X. Qian, H. Liu,H. Lin, N. Chen, and Y. Li, J. Phys. Chem. C 2011, **115**, 2611.

[42] X. Qian,H. Liu,Y. Guo, S. Zhu,Y. Song and Y. Li, Nanoscale Res Lett. 2009, 4, 955.

[43] N. S. Xu, Y. Chen, S. Z. Deng, J. Chen, X. C. Ma, E. G. Wang, J. Phys. D: Appl. Phys. 2001, **34**, 1597.

[44] E. A. Lawton, J. Phys. Chem., 1958, **62**, 384.

[45] L. Zhang, K. Wang, X.Qian, H. Liu, Z. Shi, ACS Appl. Mater. Interfaces 2013, **5**, 2761.

[46] R. Miller, Y. Y. Lau, J. H. Booske, Appl. Phys. Lett. 2007, **91**, 074105.

Figure Caption:

Figure 1: (a) FTIR spectra of CuPc nanotubes; (b) XPS survey scan of CuPc nanotubes; (c) & (d) high resolution spectra of Cu 2p doublet and N 1s respectively.

Figure 2: (a) FESEM images of CuPc nanotubes with magnified insets. (b) TEM images of a single nanotube at different magnification.

Figure 3: Schematic formation process of CuPc nanorods, half tubular structure, and nanotube.

Figure 4: FESEM images of CuPc nanotube formation mechanism.

Figure 5: (a) Current density (J) versus applied field (E) plot of CuPc nanotube at various inters electrode distances and inset of this figure indicates the J-E curve in the lower field region. (b) F-N plot of CuPc nanotube at different cathode anode distance. (c) Variation of Turn-on filed and enhancement factor with respect to the inter electrode distance. (d) Field emission stability test of CuPc nanotube at 180 μm anode-cathode distance.

Figure 6: (a-d) Three dimensional perspective of the models of a single hollow CuPc nanotube at 90^0, 60^0, 30^0 and 3^0 inclinations along with computed electric field distribution as overlay.

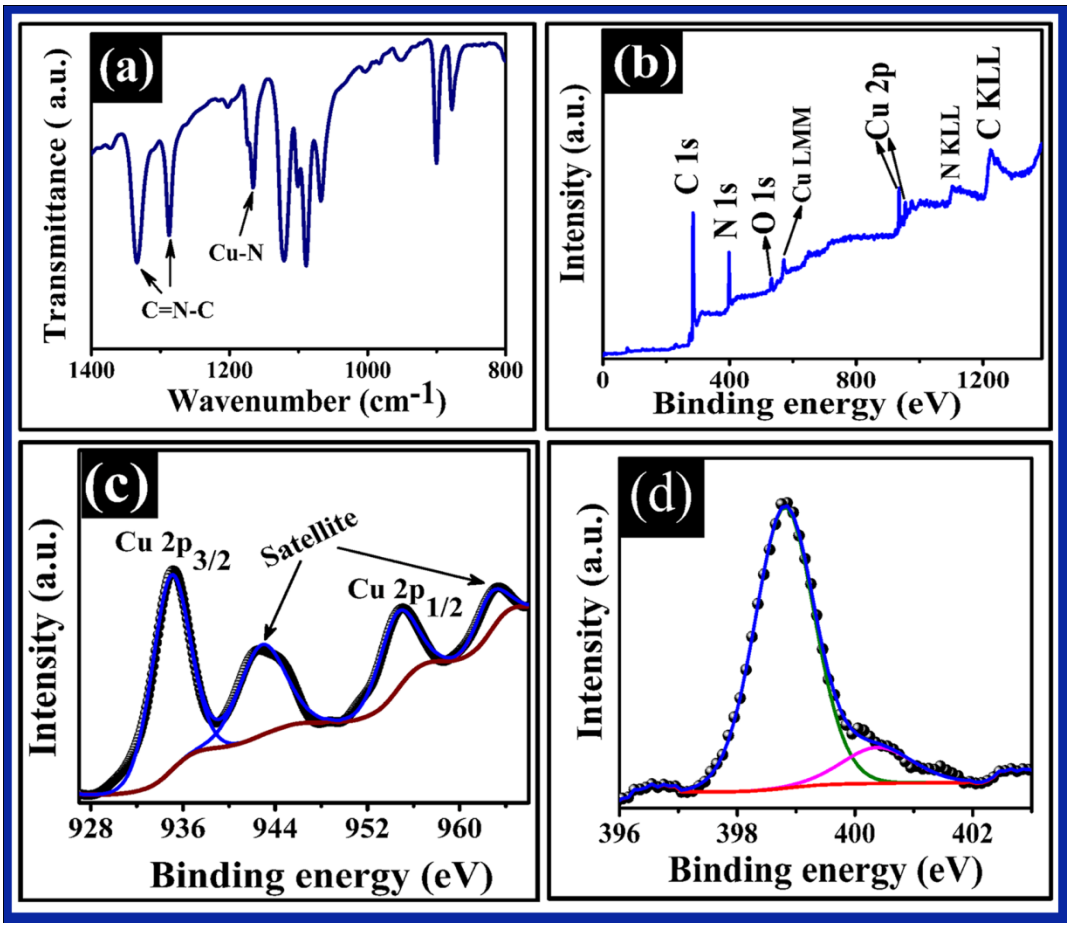

Figure: 1

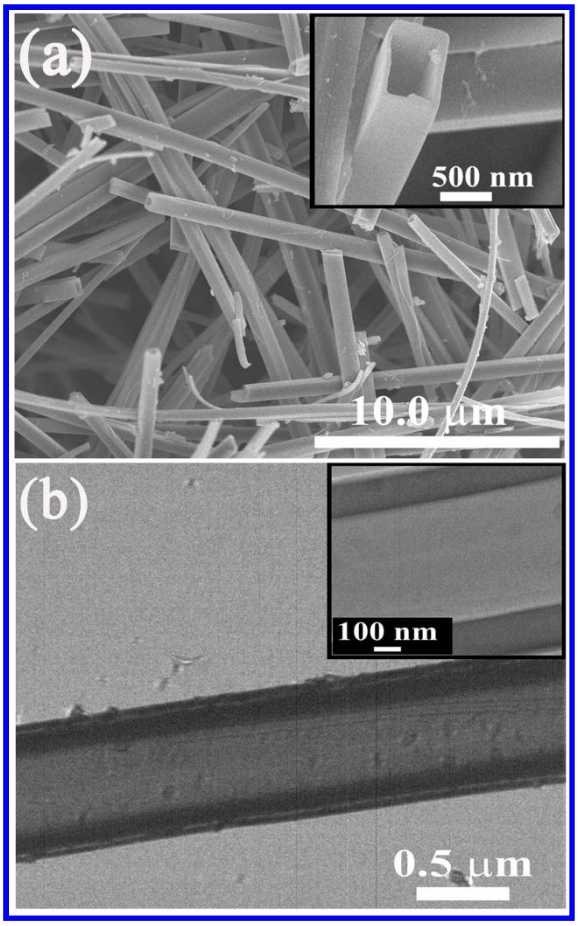

Figure: 2

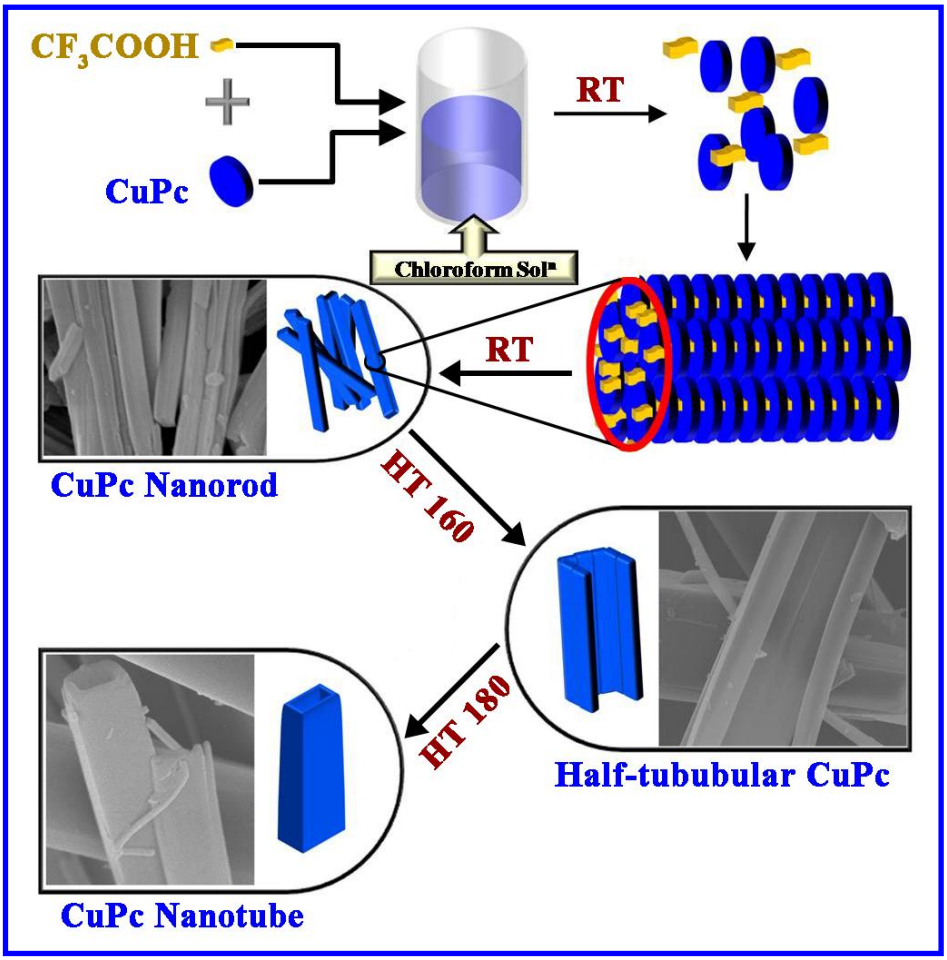

Figure: 3

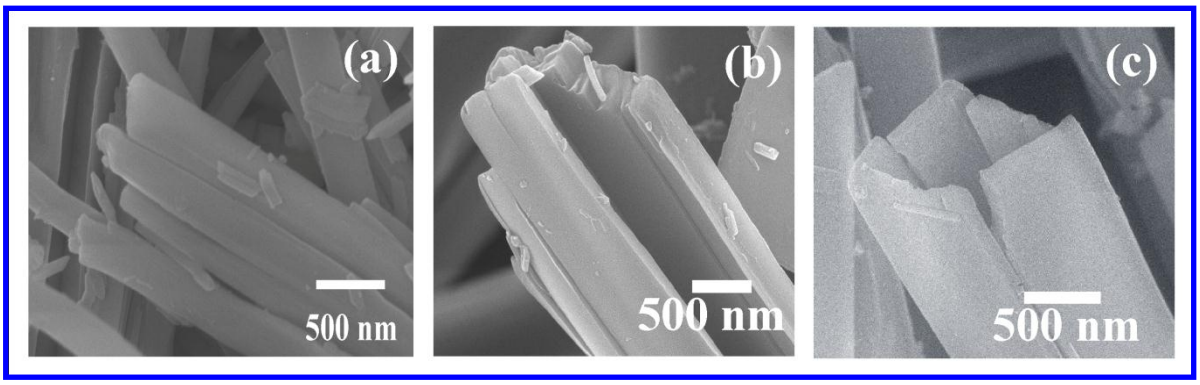

Figure: 4

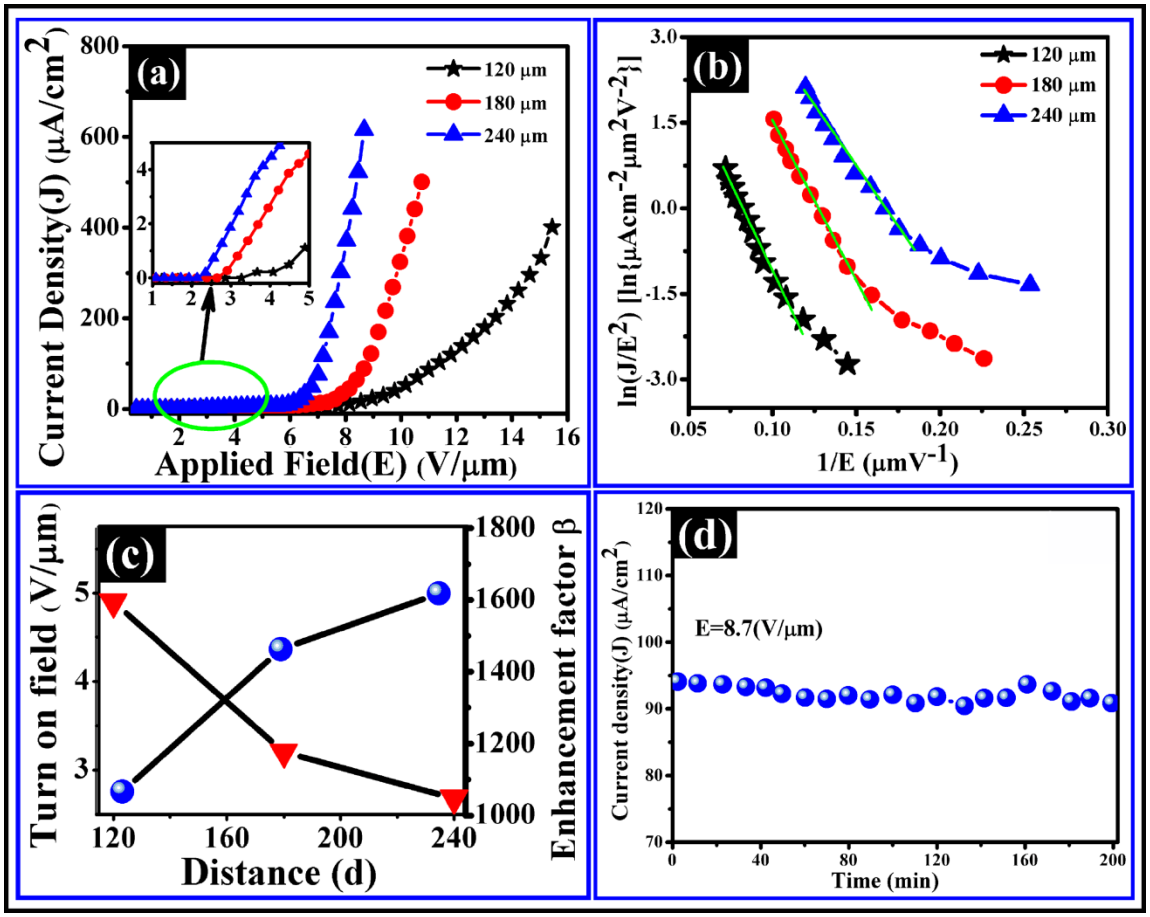

Figure: 5

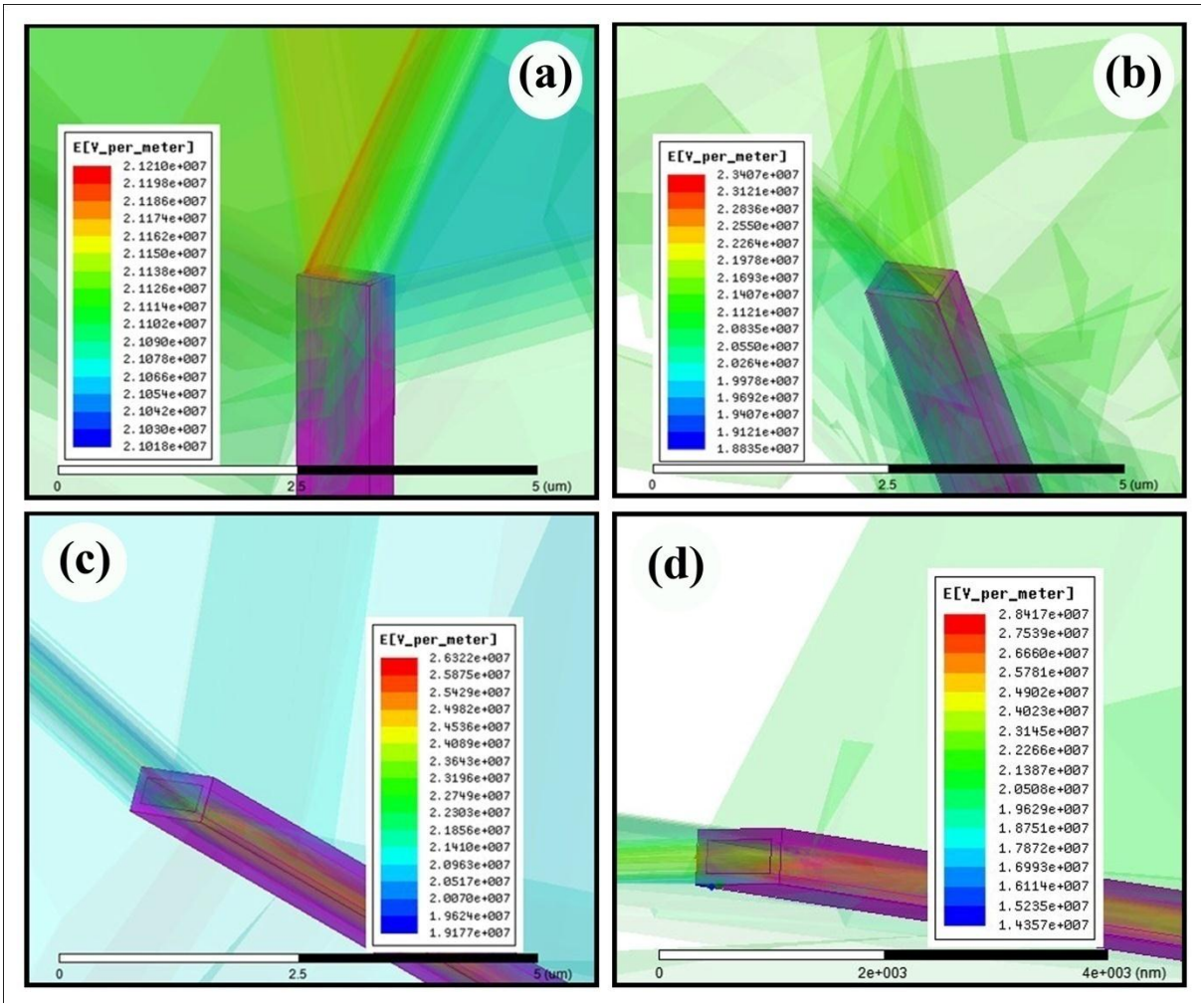

Figure: 6

Graphical Abstract:

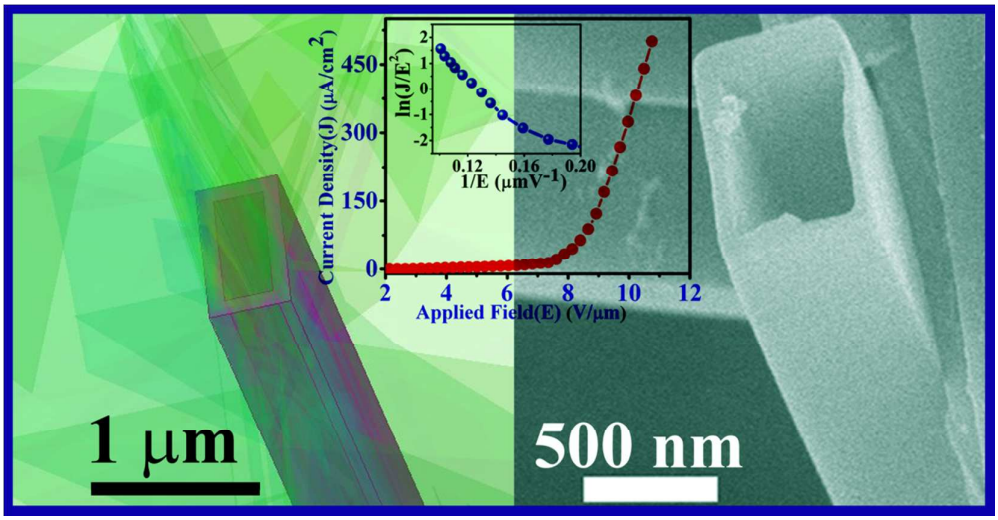

Experimentally observed excellent cold cathode emission characteristics of chemically synthesized CuPc nanotubes and theoretical justifications via finite element method simulation.